**Phycologia**
March 2018, Volume 57 Issue 2 Pages 179-190
http://dx.doi.org/10.2216/17-76.1
http://archimer.ifremer.fr/doc/00419/53089/




# *Adenoides sinensis*, a new sand-dwelling dinoflagellate species from China and reexamination of *Adenoides eludens* from an Atlantic strain

Gu Haifeng [1, *], Li Xintian [1], Chomérat Nicolas [2], Luo Zhaohe [1], Sarno Diana [3], Gourvil Priscilla [4], Balzano Sergio [4], Siano Raffaele [5, *]

[1] Third Institute of Oceanography, State Oceanic Administration, Xiamen 361005, China
[2] Ifremer, LER BO, Station de Biologie Marine, Place de la Croix, BP40537, F-29185 Concarneau Cedex, France
[3] Stazione Zoologica Anton Dohrn, Department of Integrative Marine Ecology, Villa Comunale, 80121 Naples, Italy
[4] CNRS, UMR7144, Station Biologique de Roscoff, 29680, Roscoff, France
[5] Ifremer – Centre de Brest, DYNECO PELAGOS, F-29280 Plouzané, France

* Corresponding authors : Haifeng Gu, email address : guhaifeng@tio.org.cn ; Raffaele Siano, email address : Raffaele.Siano@ifremer.fr

**Abstract :**

The sand-dwelling dinoflagellate genera *Adenoides* and *Pseudadenoides* are morphologically very close but distinct in their molecular phylogeny. We established three cultures by isolating single cells from sand samples collected in intertidal zones of Qingdao (Yellow Sea), Dongshan (South China Sea) and Brittany (English Channel, North Atlantic, France). Strain morphology was examined with light and scanning electron microscopy, and both large subunit ribosomal DNA (LSU rDNA) and small subunit ribosomal DNA (SSU rDNA) sequences were amplified. Molecular phylogeny, corroborated by morphological examination showing the existence of a ventral pore, confirmed the identification of the French strain (RCC1982) as *Adenoides eludens*. The Chinese strains differed from *Adenoides eludens* in two additional posterior intercalary plates and differed from *Pseudadenoides* in one additional apical plate having the plate formula of Po, Cp, X, 5′, 6″, 4S, 5‴, 5p, 1⁗ or alternatively Po, Cp, X, 5′, 6″, 5S, 5‴, 3p, 2⁗. Maximum likelihood and Bayesian inference, carried out with concatenated LSU and SSU sequences, demonstrated that the Chinese strains were closely related but different from *A. eludens* and, in corroboration with morphological evidence, supported their classification as a distinct species, *Adenoides sinensis sp. nov*. Morphological and molecular results confirmed the close relationship between the two genera *Adenoides* and *Pseudadenoides*.

**Keywords** : *Amphidinium eludens*, *Amphidinium kofoidii*, Benthic dinoflagellates, Molecular phylogeny, Pseudadenoides

## INTRODUCTION

The taxonomic history of *Adenoides* dates back to the pioneering work on benthic dinoflagellates by Herdman (1922). She described two sand-dwelling species, *Amphidinium eludens* Herdman and *Amphidinium kofoidii* Herdman collected at Port Erin beach, UK (illustrated in Herdman 1922, Fig. 1 and Fig. 2). Both had a minute epitheca, the latter species having a slightly larger one (Herdman 1922). Herdman (1922) also described *Amphidinium kofoidii* var. *petasatum* Herdman (illustrated in Herdman 1922, Fig. 3), which had a more pronounced epitheca. Thecal plates were not examined at that time, and these taxa were only separated on the basis of their general morphology. Later, Balech (1956) investigated some material collected at Roscoff, France, which he considered morphologically similar to *Amphidinium kofoidii* having the distinctive epitheca and a pyrenoid with a starch ring. After examining the plate pattern (1′, 4″, 5c, 4s, 5‴, 5p, 1⁗) he erected the genus *Adenoides* Balech, designating *Adenoides eludens* as type species. Dodge (1982) transferred *Amphidinium kofoidii* into *Adenoides* as *A. kofoidii* without making additional observations. Subsequently, Dodge & Lewis (1986) examined *Adenoides kofoidii*-like cells from Roscoff using SEM but called it *Adenoides eludens*, on the basis that these two species might be conspecific, as previously considered by Balech (1956). Dodge & Lewis (1986) interpreted the plate pattern of *A. eludens* (=*A. kofoidii*) as Po, 3′, 5c, 6s, 4‴, 5p, 1⁗. Hoppenrath *et al.* (2003) investigated *A. eludens sensu* Dodge & Lewis (1986) from the North German Wadden Sea using SEM pictures, and provided two interpretations of the plate patterns: Po, 4′, 6c, 4s, 5‴,

5p, 1′′′′ or Po, 4′, 6c, 5s, 5′′′, 3p, 2′′′′. Many studies were carried out on strains identified as *A. eludens*-like, until the taxonomy of this species was clarified by Gómez *et al.* (2015) using new samples from Wimereux (English Channel, France). Gómez *et al.* (2015) showed that *A. eludens sensu* Balech did not have a girdle similar to *A. kofoidii* and argued that *A. eludens sensu* Dondge & Lewis (1986) and Hoppenrath *et al.* (2003) were erroneously classified. Based on new morphological and genetic evidence, Gomez *et al.* (2015) established the genus *Pseudadenoides* F.Gómez, R.Onuma, Artigas & Horiguchi to include *P. kofoidii* comb. nov. formerly classified as *A. kofoidii*. Apart from the absence of a girdle in *A. eludens*, the two genera also differ in the number of apical plates, that is five in *Adenoides* and four in *Pseudadenoides* (Gómez *et al.* 2015). Recently, a new *Pseudadenoides* species, *P. polypyrenoides* Hoppenrath, Yubuki, R.Stern & B.S.Leander, was described. This species is genetically different from *P. kofoidii* on the basis of small subunit ribosomal DNA (SSU rDNA) and large subunit ribosomal DNA (LSU rDNA) sequences. In addition, the number and size of pyrenoids, the location of nucleus and the number of large pores on the hypotheca differ between the two species (Hoppenrath *et al*. 2017).

Here we report a new *Adenoides* species from Chinese waters, based on detailed morphological observations and molecular phylogeny built using concatenated data from SSU and LSU rDNA sequences. In addition, we reexamined a French strain of *A. eludens* isolated from north Atlantic waters (English Channel). These observations contributed to a better definition of morphological features that are common to species of *Adenoides* and allow their distinction from *Pseudadenoides.*

## MATERIALS AND METHODS

Chinese strains were collected nearby Qingdao (Yellow Sea, 36°3.115′ N, 120°21.827′″ E) and Dongshan (South China Sea, 23°36.102′ N, 117°25.269′ E) during low tide on October 14, 18, 2015, respectively. The superficial sandy sediments were collected with a spoon and put into a plastic bottle together with local seawater. Individual cells were isolated from the sediment samples using an inverted microscope AE31 (Motic, Xiamen, China) with a micropipette into 96 well plates, with each well containing 300 µl f/2-Si medium (Guillard & Ryther 1962). The plates were incubated at 20°C, 90 µmol photons · $m^{-2}$ · $s^{-1}$ with a light: dark cycle of 12:12 h, and examined daily with the above inverted microscope. Two strains (TIO303, TIO308) of *Adenoides* from Qingdao and Dongshan, respectively were established and used for subsequent examinations. These two strains are now lost.

The French strain was obtained by micropipette isolation of a single cell present in sediments collected in Santec beach (48°42′ N, 4°12′ W) (Britanny, English Channel, France). The resulting monoclonal culture was maintained in filter-sterilized seawater with f/2 (Sigma G9903) at 15°C with an irradiance of 100 µmol photons · $m^{-2}$ · $s^{-1}$ in a 12:12 light: dark regime. The culture was deposited in the Roscoff culture collection (Roscoff Culture Collection, http://www.sb-roscoff.fr/Phyto/rcc) as RCC1982.

Live cells of Chinese strains TIO303 and TIO308 were examined and photographed using a Zeiss Axio Imager microscope (Carl Zeiss, Göttingen, Germany)

equipped with differential interference contrast and a Zeiss Axiocam HRc digital camera. To observe the shape and location of the nucleus, cells were stained with 1:100,000 Sybr Green (Sigma Aldrich, St. Louis, MO, USA) for 1 min, and photographed using the Zeiss fluorescence microscope with a Zeiss-38 filter set (excitation BP 470/40, beam splitter FT 495, emission BP 525/50).

Forty cells of strain TIO303 were measured using scanning electron microscopy (SEM). For SEM observation , cells were fixed in 2.5% glutaraldehyde in 0.1 M sodium-phosphate buffer (pH 7.4) at 20°C for 1 h. They were transferred to a coverslip coated with poly-L-lysine (molecular weight 70,000–150, 000) for 30 min and then washed for 10 min in a 1:1 solution of distilled water and filtered seawater, followed by a second wash in distilled water for 10 min. The samples were then dehydrated in a series of ethanol (10, 30, 50, 70, 90% and 100% (three times), 10 min at each step), critical point dried (K850 Critical Point Dryer, Quorum/Emitech, West Sussex, UK), sputter-coated with gold, and examined using a Zeiss Sigma FE (Carl Zeiss Inc., Oberkochen, Germany) scanning electron microscope.

Live cells of strain RCC1982 were observed and measured with a Zeiss Axiophot direct light microscope (Carl Zeiss, Oberkochen, Germany). Light micrographs were taken with a Zeiss AxioCam digital camera system (Carl Zeiss, Oberkochen, Germany). For SEM observations culture subsamples were fixed with formol (2% final concentration), placed on a Nuclepore (Nuclepore, Pleasanton, CA, USA) polycarbonate filter, dehydrated in an ethanol series (25%, 50%, 75%, 95%, 100%) and critical point dried. The filter was mounted on a stub, sputter coated with gold and

examined with a JEOL JSM-6500F SEM (JEOL-USA Inc., Peabody, MA, USA). The Kofoidian system alone and combined with the Taylor-Evitt system were used for the designation of the thecal plates numbering of all strains (Fensome *et al.* 1993).

Individual cells of strains TIO303 and TIO308 were rinsed several times in sterilized distilled water, broken by squeezing the coverslip above, and then transferred into a PCR tube. Four cells were used as the template to amplify about 1430 bp of the LSU rRNA gene (D1-D6 domains) and 1740 bp of the SSU rRNA gene, using the primers D1R (forward, 5′-ACCCGCTGAATTTAAGCATA-3′) (Scholin *et al.* 1994), 28-1483R (reverse, 5′-GCTACTACCACCAAGATCTGC-3′) (Daugbjerg *et al.* 2000), SR1(forward, 5′-TACCTGGTTGATCCTGCCAG-3′) and SR12b (reverse, 5′-CGGAAACCTTGTTACGACTTCTCC-3′) (Takano & Horiguchi 2006). A 50 µL PCR cocktail containing 0.2 µM forward and reverse primer, PCR buffer, 50 µM dNTP, 1U of Taq DNA polymerase (Takara, Dalian, China) was subjected to 35 cycles using a Mastercycler PCR (Eppendorf, Hamburg, Germany). The PCR protocol was identical to that of Liu *et al.* (2015a).

For strain RCC1982, DNA was extracted as described previously (Balzano *et al.* 2012): 2 ml of exponentially growing culture were collected, centrifuged at 11 000 rpm for 10 min and 1.8 ml of supernatant removed. Genomic DNA was then extracted using Qiagen Blood and Tissue kit. 200 µl ATL buffer (Qiagen Blood and Tissue kit) and 20 µl of 20 mg $ml^{-1}$ lysozyme (Sigma Aldrich Chimie S.a.r.l. Lyon, France) were added to 200 µl of cultures. Samples were incubated for 30 min at 37°C, then, 200 µl of AL buffer (Qiagen Blood and Tissue kit), 75 µl of 20 mg $ml^{-1}$ proteinase K

(Sigma-Aldrich Chimie S.a.r.l. Lyon, France) and 20 µl glycogen (Applied Biosystems, Foster city, USA) were added and samples were incubated at 56°C for 30 min. Proteinase K was then inactivated by incubating samples at 75°C for 10 min. 200 µl of absolute ethanol (Fisher Bioblock Scientific, Illkirch, France) were added and samples were transferred into filter columns (Qiagen Blood and Tissue kit) and centrifuged at 8,000 rpm for 1 min. Filtrate was then discarded and washed twice with 500 µl buffers AW1 and AW2 (Qiagen Blood and Tissue kit), respectively. DNA was then eluted from the filters by adding 50 µl buffer AE (Qiagen Blood and Tissuekit), incubating samples for 3 min and centrifuging them at 14,000 rpm for 1 min.

Both the SSU and LSU rRNA gene were then amplified by PCR. For both amplifications 1 µl of genomic DNA was mixed with 0.5 µl 10 µM solution of both forward and reverse primers, 15 µl of HotStar Taq Plus Master Mix Kit (Qiagen, Courtaboeuf, France), 3 µl of Coral Load (Qiagen, Courtaboeuf, France) and Milli-Q water up to a final volume of 30 µl. For the SSU rRNA gene, primers 63f (5'-ACGCTTGTCTCAAAGATTA-3') and 1818r (5'-ACGGAAACCTTGTTACGA-3') were used (Lepère *et al*. 2011) and PCR reactions were as follows: an initial incubation step at 95°C during 5 min, 35 amplification cycles (95°C for 1 min, 57°C for 1 min 30 sec, and 72°C for 1 min 30 sec) and a final elongation step at 72°C for 10 min. The LSU rRNA gene was amplified using primers D1R (ACCCGCTGAATTTAAGCATA) and D3Ca (ACGAACGATTTGCACGTCAG) targeting the D1-D3 region of the nuclear LSU rDNA (Lenaers *et al*. 1989) and PCR reactions were performed with 30 amplification

cycles of 94°C for 1 min, 5°C for 1 min 30 sec, and 72°C for 1 min. Both SSU and LSU rRNA amplicons were purified using Exosap (USB products, Santa Clara, USA) and sequences were determined using Big Dye Terminator V3.1 (Applied Biosystems, Foster city, USA). Primers used for sequencing were the same as above as well as an internal primer Euk528f (Zhu *et al*. 2005) for the SSU rRNA gene.Both partial SSU and LSU rDNA sequences of the analyzed strains are deposited in GenBank with the accession numbers KT860567, MF535292 to MF535296, respectively.

A unique concatenated phylogeny (SSU + LSU) was constructed for strains TIO303, TIO308, and RCC182. Around 3,200 bp sequences newly obtained (including SSU and partial LSU) were first aligned with those of related species available in GenBank using 'BioEdit' v7.0.0 (Hall 1999), and then using Mafft (Katoh *et al.* 2005) (http://mafft.cbrc.jp/alignment/server/). *Noctiluca scintillans* (Macartney) Kofoid & Swezy was selected as the outgroup. The optimal model was chosen using JmodelTest (Posada 2008). A general time reversible model (GTR +G) was selected with Akaike information criterion. Maximum likelihood-based analyses were conducted with 'RAxML' v7.2.6 (Stamatakis 2006) using the best-fitting substitution model on the T-REX web server (Boc *et al.* 2012). 500 bootstraps were carried out. A Bayesian reconstruction of the data matrix was performed with MrBayes 3.0b4 (Ronquist & Huelsenbeck 2003) using the best-fitting substitution model. Four Markov chain Monte Carlo (MCMC) chains ran for ten millions generations, sampling every 1,000 generations with a burn in of 10%. A majority rule consensus tree was created in order to examine the posterior probabilities of each

clade.

## RESULTS

Both morphological and phylogenetic analyses allowed the description of *A. sinensis* sp. nov. H. Gu, X. Li & Z. Luo for strains TIO303 and TIO308, and the identification of RCC1982 as *A. eludens* Balech, for which new morphological and comparative information are provided.

### *Adenoides sinensis* sp. nov. H.Gu, X.Li & Z.Luo

Figs 1–21

DIAGNOSIS: Motile cells 34.1–54.8 µm long, 14.7–24.2 µm wide, and 27.7–41.5 µm deep. Cells flattened in dorsal-ventral view with a minute epitheca. Plate tabulation Po, Cp, X, 5′, 6″, 4S, 5‴, 5p, 1⁗ or alternatively Po, Cp, X, 5′, 6″, 5S, 5‴, 3p, 2⁗. A ventral pore present at the junction of pore plate and plates 4′, 5′.

HOLOTYPE: SEM stub from strain TIO303, designated as TIO201702 and deposited at Third Institute of Oceanography, State Oceanic Administration, Xiamen 361005, China.

TYPE LOCALITY: Qingdao, Yellow Sea (36°3.115′ N, 120°21.827′ E). Collection date: October 14, 2015.

ETYMOLOGY: '*sinensis*' is derived from China and refers to the geographic area where the species is distributed.

HABITAT: intertidal, sand-dwelling.

GENBANK ACCESSION NUMBERS: MF535292, MF535295, the nuclear-encoded

LSU and SSU rDNA gene sequence of strain TIO303.

Cells of strain TIO303 were ellipsoidal and flattened in dorsal-ventral view (Fig. 1). They were 34.1–54.8 µm (average 42.2 ± 5.0 µm, n = 40) long, 14.7–24.2 µm (average 20.3 ± 2.8 µm, n = 19) wide, and 27.7–41.5 µm (average 32.6 ± 3.8 µm, n = 21) deep. The epitheca was minute and button like (Figs 2, 3). The cells contained green to brown chloroplasts near the cell surface (Figs 1–5). The transverse flagellum was at the end of the epitheca, completely encircling the cell (Fig. 3). The longitudinal flagellum trailed behind the cell (Fig. 2). At times several starch granules were visible (Figs 4, 5). A pyrenoid was not observed. The nucleus was curved, located in the middle of the cell and displaced toward the dorsal end (Fig. 6). The cells swam slowly forward accompanied by rotations.

The apical pore was rounded (1.4–2.0 µm wide (average 1.6 ± 0.4 µm, n = 8)), located in the middle of the pore plate (Po), and covered by a cover plate (Cp) (Figs 7–10). There were 12–15 pores evenly distributed near the margins of the pore plate (Figs 7, 8). The apical pore was connected through a finger-like protrusion to the small canal plate (X), which slightly invaded the first apical plate (1′) (Fig. 8). Plate 1′ was four sided, narrow and elongated (Fig. 9). Plate 2′ was four-sided and much smaller than the other apical plates, whereas plate 5′ was six-sided and the largest (Fig. 7). Plates 3′ and 4′ were five-sided and median in size (Figs 7–9). A pronounced ventral pore (ca. 0.3 µm wide) was observed at the junction of the pore plate and

plates 4′, 5′ (Fig. 7, seven cells out of eight), but its position could change to the middle of plate 4′ (Fig. 8, one cell out eight). There were six precingular plates which were similar in size except that 6″ was much smaller (Figs 7, 9, 10). The sulcus was excavated and slightly intruded the epitheca (Figs 9, 11). The sulcus consisted of an anterior sulcal plate (Sa), a left sulcal plate (Ss), a right sulcal plate (Sd) and a posterior sulcal plate (Sp) (Fig. 11). Plate Sd was four-sided and the smallest, whereas plate Ss was six-sided and the largest (Fig. 12). Two flagellar pores were situated among the four sulcal plates (Fig. 11).

The hypotheca consisted of five postcingular, five posterior intercalary plates and one antapical plate (Figs 13–20). The fifth postcingular plate (5‴) was four sided and the smallest (Fig. 13). Plates 1‴ and 3‴ were pentagonal and symmetrical, whereas plates 2‴ and 4‴ were five sided and asymmetrical (Figs 14–18). Plates 2p and 5p were large and irregular, occupying most part of the left and right side of the hypotheca, respectively (Figs 15, 18). Plates 3p and 4p were smaller and pentagonal, situated in the dorsal part (Figs 15–17). Plate 1p was five sided and median in size (Figs 13, 14). There was only one pentagonal antapical plate (Figs 19, 20).

All thecal plates were smooth with scattered pores, except several plates in the sulcal area (Fig. 11). The sutures among plates were generally wide and transversely striated (Figs 7, 15, 18). At the junction of plates 3p, 4p and 1‴′, there were small areas of dense pores, comprising ca. 20 pores (Fig. 21). The plate formula is designated as Po, Cp, X, 5′, 6″, 4S, 5‴, 5p, 1‴′ according to the Kofoid system or Po, Cp, X, 5′, 6″, 5S, 5‴, 3p, 2‴′ after the Kofoid combined with the Taylor-Evitt system.

The alternative tabulations are simply based on different interpretations rather than plate variability. Strain TIO308 shared identical morphology with that of TIO303 (Figs S1–S6).

***Adenoides eludens* Balech**

Cells of strain RCC1982 were oval, flattened laterally, 28–33 μm long (average 31.4 ± 1.6 μm, n = 20), 22–26 μm wide (average 24.2 ± 1.4 μm, n = 20), 16–21 μm deep (average 18.6 ± 1.8 μm, n = 10), with a length to width ratio of 1.3 and a length to depth ratio of 1.7. The epitheca was smaller and narrower than the hypotheca, giving the cell a typical asymmetrical shape in lateral view. Flagella both emerged from the ventral sulcal indentation, sometimes both were spread out of the cell, and other times one flagellum encircled the cell (Figs S7, S8). A large oval to round nucleus was posterior and surrounded by several granules, probably of lipidic material (Fig. S7). Two oval pyrenoids were present in the cell. In lateral view, one pyrenoid was visible in the centre of the cell, above the nucleus, while from the dorsal or ventral side, the two pyrenoids were both visible close to the thecal margins (Fig. S9). On occasion, a large round food vacuole was also visible above or laterally to the pyrenoid. A single chloroplast was present in the cell and appeared as a reticulated structure after blue-light excitation (Fig. S10). No stigma was detected.

Precingular plates (6″) were pentagonal, with the exception of the plates 4″ and 6″ which were four-sided (Figs 22–26). Located between 5″ and Sa, plate 6″ was in contact with 5‴ in the posterior part and with 1′ in the anterior part (Fig. 26). Plate 6″

was generally very slender, however it was rather large in some specimens. This plate is assigned to the precingular series considered the presence of pores like other precingular plates and different from sulcal ones.

The apical pore complex (APC) was composed of a horseshoe-shaped apical pore plate (Po) with 10–17 pores, an oval cover plate (Cp) surrounded sometimes by a coiled ring and a rectangular canal plate (X) (Figs 27–29). Five apical plates (1′–5′) encircled the APC. Plate 1′ was triangular, longer than wider and the other apical plates were quadrangular. Plate 1′ can be raised to form the thecal edge, because of a greater development of plate's margins. This plate alteration gave the cell a peculiar irregular shape, also visible in light microscopy. A peculiar ventral pore (ca. 0.3 μm wide) was observed at the junction of Po, 4′ and 5′ plates (Figs 27, 28), but its position was sometimes more dorsal in the middle of plate 4′ (Fig. 29). The sulcus occupied about the half of the cell length. It was composed of four plates, one anterior (Sa), a right (Sd) and a left (Ss) sulcal plate, and the posterior sulcal (Sp) (Figs 26, 30). The 1‴ was longer than the other plates of the series, and contacted the antapical plate (1⁗) (Figs 22–24). Plate 2‴ was pentagonal and located on the left lateral side of the theca. It was ventrally in contact with the left sulcal plate (Fig. 24). Plate 3‴ was dorsal and five-sided (Figs 22, 23). Plate 4‴ was the largest of the series, occupying most of the right hypotheca, and it was pointed towards the dorsal part of the cell (Fig. 23). The 5‴ plate was the smallest of the series, contacting the 5″ and the 6″ anteriorly, and the 4p, posteriorly. In some specimens, this plate was found to be split in two smaller plates (Fig. 26). Three pentagonal plates (3p) were also present in the

hypotheca, located between the postcingular series and the antapical plate. The 1p plate was present in the left side of the hypotheca, was large and pointed towards the antapex (Fig. 22). The 2p plate was on the dorsal and right sides of the cell, whereas the 3p was on the right lateral side, and at the lower side of the 4‴ (Fig. 23). A single antapical plate (1⁗) was present and four-sided (Figs 22–24). Plates were smooth, with several pores scattered along plate margins, with the exception of Cp, X, sulcus and precingular plates devoid of pores. At the dorsal antapex, pore fields were present in the antapical part of 1p, 2p and 1⁗ plates (Fig. 23).

The schematic interpretations of thecal plates of *Adenoides sinensis* and *A. eludens* are shown in Figs 31–40.

**Molecular character and phylogeny**

Sequence similarities between species of the closely related genera *Adenoides* and *Pseudadenoides* are provided in table S1. The best phylogenetic tree constructed by Bayesian inference (BI) with the concatenated SSU and LSU sequences is illustrated in Fig. 41. Maximum likelihood (ML) generated a similar topology differing only in a few internal nodes. *Adenoides sinensis* grouped together with *Adenoides* sp. (strain NIES-1402) with maximal support (BI posterior probability: 1.0 /ML bootstrap: 100) and formed a sister clade of *A. eludens* with moderate support (BI posterior probability: 0.81/ML bootstrap: 100). These two clades were sister to a clade including *Pseudadenoides kofoidii* and *P. polypyrenoides* with maximal support. The *Adenoides*/*Pseudadenoides* group was a sister clade of Prorocentrales with moderate

support (BI posterior probability: 0.81/ML bootstrap: 100).

## DISCUSSION

The analysis of the thecal plates in *Adenoides* is difficult. The sixth cingular plate has been designated as the anterior sulcal plate (Dodge & Lewis 1986), and the number of antapical plates can vary from one to two according to different interpretations (Hoppenrath *et al.* 2003). For clarity, we tried to follow the Kofoid system for comparisons and discussions below.

Within the dinoflagellate lineage the number of intercalary plates can vary at the intrageneric level. For instance, *Protoperidinium* Bergh incorporates species with one, two or three anterior intercalary plates (Faust 2006; Liu *et al.* 2015b); and *Azadinium* Elbrächter & Tillmann also encompasses species with two or three anterior intercalary plates (Luo *et al.* 2013; Tillmann *et al.* 2014). Instead, the number of apical plates appears much more conservative within a genus. Considering the conservation of this morphological character, and in the light of a genetic support, we preferred describing a new species within *Adenoides* instead of *Pseudadenoides*. *Adenoides sinensis* differs from *Pseudadenoides* in the number of apical plates (5 versus 4) and differs from *Adenoides eludens* in the number of posterior intercalary plates (5 versus 3). As a consequence, the genus *Adenoides* needs emendation to incorporate the new species, here described as *Adenoides sinensis* (strains TIO303 and TIO308).

In the light of our new morphological observations, some morphological characters used to distinguish *Adenoides* and *Pseudadenoides* seem no longer valid.

The absence of a girdle was regarded as a key character to differentiate *Adenoides* from *Pseudadenoides* (Gómez *et al.* 2015). Girdle absence is rare in dinoflagellates except in the Order Prorocentrales. In addition, an incomplete cingulum was reported in benthic species of *Amphidiniopsis* Woloszynska (Murray & Patterson 2002) and *Herdmania* Dodge (Hoppenrath 2000b). The pelagic family Podolampadaceae does not show an apparent cingulum, but the three plates in the equatorial part are the homologues of cingular plates of other dinoflagellates (Carbonell-Moore 1994). Gómez *et al.* (2015) illustrated a transverse flagellum encircling the cell in *Adenoides eludens*, but did not point out its location clearly. In the original descriptions of *A. eludens*, Herdman (1922) mentioned that the cell has a girdle where the transverse flagellum is located. We considered that *Adenoides* has a "depressed" cingulum like *P. kofoidii* and *P. polypyrenoides*, thus cingular plates are homologous in *Adenoides*/*Pseudadenoides*, and their separation in different series, as interpreted by Gomez *et al*. (2015), seems artificial.

Our results show that the presence of posterior intercalary plates surrounding the antapical plate is shared by both *Adenoides* and *Pseudadenoides*. Thus this character might not be considered as a generic distinguishing feature, as suggested by Hoppenrath *et al*. (2017).

The thecal pores can play an important role in the process of absorption and excretion metabolism (Balech 1980), but the taxonomic value of these pores is largely unknown. Both *Adenoides eludens* and *A. sinensis* have at least 10 pores at the margins of the pore plates, whereas *Pseudadenoides polypyrenoides* and *P. kofoidii*

only have five and seven pores (Gómez *et al.* 2015; Hoppenrath *et al.* 2017; present study). Such pores were also reported in some species of *Thecadinium* Kofoid & Skogsberg, suggesting that they could be useful for species differentiation (Hoppenrath 2000a). Dense pore assemblages were observed in the hypothecal plates (e.g. the antapical plate) in specimens of *Adenoides* (Gómez *et al.* 2015; present study), but not in *Pseudadenoides* (Hoppenrath *et al.* 2003; Gómez *et al.* 2015). Such pore disposition was also observed in *Rhinodinium* Murray, Hoppenrath, Yoshimatsu, Toriumi & Larsen (Murray *et al.* 2006), and *Azadinium* (Tillmann *et al.* 2016), and might not be a significant distinguishing character at generic level.

The morphological observations obtained here on three new *Adenoides* strains allow us to identify the ventral pore as a character distinguishing *Adenoides* from *Pseudadenoides.* A ventral pore was found in *A. sinensis* and *A. eludens*, but not in *Pseudadenoides kofoidii* and *P. polypyrenoides* (Hoppenrath *et al.* 2003 (as *A. eludens*); Gómez *et al.* 2015; Hoppenrath *et al.* 2017). A ventral pore was always found in *Azadinium* species and is an important taxonomic character within this genus (Tillmann *et al.* 2014). The functional role of the ventral pore, however, is not clear. Two and three large pores (about 0.6 µm in diameter, twice the size of the ventral pore in *Adenoides sinensis*) were present in *Pseudadenoides kofoidii*, located in the third and fourth posterior intercalary plates, through which mucus secretion was observed (Hoppenrath *et al.* 2003) and in *P. polypyrenoides*, located in the third and fourth posterior intercalary plates and the antapical plate (Hoppenrath *et al.* 2017). Whether these large pores are diagnostic for *Pseudadenoides* remain to be

determined.

*Adenoides eludens* was reported from Port Erin, UK (Herdman 1922), Wimereux and the English channel, France (Gómez *et al.* 2015; present study), whereas *Pseudadenoides kofoidii* appears to have a wider distribution, reported in Port Erin, UK (Herdman 1922), Roscoff, France (Balech 1956; Dodge & Lewis 1986), Canada, and the German Wadden Sea (Hoppenrath *et al.* 2003; Hoppenrath *et al.* 2017). A specimen from Izu Peninsula, Japan, attributed to *Adenoides eludens* (fig. 11 in Hara & Horiguchi 1982) shows an obvious epitheca and differ from *A. sinensis* in the shape of plate 4′ (Hara & Horiguchi 1982). The lower, left side of the plate 4′ is much longer than that of *A. sinensis*, suggesting that the Japanese specimens might be *Pseudadenoides kofoidii*, as proposed by Hoppenrath *et al.* (2017). The Japanese strain NIES-1402 is genetically very close to *A. sinensis*, but its actual identity needs confirmation from morphological evidence. *Adenoides eludens* was also reported from Kuwait (Saburova *et al.* 2009). The specimens described have a minute epitheca and a larger posterior intercalary plate, likely being a novel species. *Pseudadenoides polypyrenoides* is only known fromPacific coast of Canada (Hoppenrath *et al.* 2017).

The phylogenetic position of *Adenoides eludens* was reported for the first time by Saldarriaga *et al.* (2001) based on SSU rDNA sequences. In their phylogenetic tree *A. eludens* is close to *Prorocentrum* Ehrenberg but they do not form a well-resolved clade. Zhang *et al.* (2007) demonstrated that *Prorocentrum* is monophyletic using concatenated data set from mitochondrial DNA (cob, cox1) and SSU rDNA sequences. They showed that *Adenoides* was the closest relative of *Prorocentrum*, although with

low support. Molecular phylogeny inferred from more genes including ribosomal DNA, mitochondrial DNA and proteins revealed moderate to strong support of the *Adenoides-Prorocentrum* clade (Orr *et al.* 2012).

Historically, *Adenoides* was classified in different orders, such as the Gymnodiniales and Peridiniales (Silva 1979; Dodge 1982). On the basis of morphological observations only, Hoppenrath *et al.* (2003) proposed that *Pseudadenoides kofoidii* (ex *A. eludens*) belonged to Gonyaulacales due to the lack of a canal plate, the tabulation of the sulcus and the hypotheca, and the mode of vegetative cell division. This idea was not supported by the multigene phylogeny of Orr *et al.* (2012). Later a canal plate was revealed in *Adenoides eludens* and *Pseudadenoides kofoidii* (Gómez *et al.* 2015) which do not justify the classification of *Adenoides* and *Pseudadenoides* within Gonyaulacales. Our results support the close relationship between *Adenoides* and *Pseudadenoides*, and the relationship between the *Adenoides/ Pseudadenoides* clade with *Prorocentrum* (Zhang *et al.* 2007; Orr *et al.* 2012; Hoppenrath *et al.* 2017). However, a supergeneric classification of *Adenoides* and *Pseudadenoides* appears to be premature and needs to be supported by further genetic data.

The prorocentroids, with two anterior flagella and the theca consisting mainly of two large plates (valves), have been suggested to represent the most primitive dinoflagellates (Taylor 1980) or, alternatively, the more advanced dinoflagellates (Dodge 1983). Saldarriaga *et al.* (2004) suggested that Dinophysiales/ Prorocentrales might be derived from Peridiniales. Our morphological results suggest that the genera

*Adenoides* and *Pseudadenoides* might be an intermediate link between Peridiniales and Prorocentrales.

The presence of one antapical plate is not typical of Gonyaulacales and Peridiniales, but it was reported in *Adenoides* and *Pseudadenoides*, and also in other laterally compressed, sand-dwelling species including *Thecadinium* (Hoppenrath 2000a), *Cabra* Murray & Patterson (Selina *et al.* 2015), *Ailadinium* Saburova & Chomérat (Saburova & Chomérat 2014), *Roscoffia* Balech (Balech 1956; Hoppenrath & Elbrächter 1998), *Rhinodinium* (Murray *et al.* 2006), *Sabulodinium* Saunders & Dodge (Hoppenrath *et al.* 2007). These genera are classified temporarily in different orders, suggesting that convergent evolution has occurred for adaptation to benthic habitats. New topologies based on different genes could probably demonstrate a phylogenetic relationship between those genera and help in elucidating the evolution of benthic dinoflagellates.

***Adenoides* Balech emended H. Gu, Chomérat & Siano**

DIAGNOSIS: Armoured cell laterally compressed, lacking a cingulum and with flagella inserted ventrally. Thecal plate formula Po, 5′, 6″, 0c, 3+s, 5‴, 3-5p, 1⁗, differing from *Pseudadenoides* in the number of apical plates (5 vs 4), and in the presence of a ventral pore in the apical plate series.

TYPE SPECIES: *Adenoides eludens* (Herdman) Balech.

BASIONYM: *Amphidinium eludens* Herdman 1922, p. 22, fig. 1.

SYNONYM: *Adenoides kofoidii* sensu Dodge 1982.

SPECIES DESCRIBED: *Adenoides eludens, Adenoides sinensis*

**ACKNOWLEDGEMENTS**

We thank two anonymous reviewers for constructive suggestions that improved the manuscript greatly. This project was supported by the National Key Research and Development of China (2017YFC1404303) and National Natural Science Foundation of China (41676117). ASSEMBLE EU FP7 Research Infrastructure Initiative (EU-RI-227799) funded RS research.

**REFERENCES**

BALECH E. 1956. Étude des dinoflagellés du sable de Roscoff. *Revue Algologique, Nouvelle Serie* 2: 29–52.

BALECH E. 1980. On the thecal morphology of dinoflagellates with special emphasis on circular and sulcal plates. *Anales del Centro de Ciencias del Mar y Limnologia, Universidad Nacional Autonomia de Mexico* 7: 57–68.

BALZANO S., MARIE D., GOURVIL P. & VAULOT D. 2012. Composition of the summer photosynthetic pico and nanoplankton communities in the Beaufort Sea assessed by T-RFLP and sequences of the 18S rRNA gene from flow cytometry sorted samples. *The ISME Journal* 6**:** 1480–1498.

BOC A., DIALLO A.B. & MAKARENKOV V. 2012. T-REX: a web server for inferring, validating and visualizing phylogenetic trees and networks. *Nucleic Acids Research* 40: W573–W579.

CARBONELL-MOORE M. 1994. On the taxonomy of the family Podolampadaceae Lindemann (Dinophyceae) with descriptions of three new genera. *Review of Palaeobotany and Palynology* 84: 73–99.

DAUGBJERG N., HANSEN G., LARSEN J. & MOESTRUP Ø. 2000. Phylogeny of some of the major genera of dinoflagellates based on ultrastructure and partial LSU rDNA sequence data, including the erection of three new genera of unarmoured dinoflagellates. *Phycologia* 39**:** 302–317.

DODGE J.D. 1982. *Marine dinoflagellates of the British Isles.* Her Majesty's Stationery Office, London, 303 pp.

DODGE J.D. 1983. Dinoflagellates: investigation and phylogenetic speculation. *British Phycological Journal* 18: 335–356.

DODGE J. & LEWIS J. 1986. A further SEM study of armoured sand-dwelling marine dinoflagellates. *Protistologica* 22: 221–230.

FAUST M.A. 2006. Creation of the subgenus *Testeria* Faust *subgen. nov.* *Protoperidinium* Bergh from the SW Atlantic Ocean: *Protoperidinium novella* sp. nov. and *Protoperidinium concinna* sp. nov. Dinophyceae. *Phycologia* 45: 1–9.

FENSOME R.A., TAYLOR F.J.R., NORRIS G., SARJEANT W.A.S., WHARTON D.I. & WILLIAMS G.L. 1993. A classification of fossil and living dinoflagellates. *Micropaleontology Special Publication* 7: 1–245.

GÓMEZ F., ONUMA R., ARTIGAS L.F. & HORIGUCHI T. 2015. A new definition of *Adenoides eludens*, an unusual marine sand-dwelling dinoflagellate without cingulum, and *Pseudadenoides kofoidii* gen. & comb. nov. for the species formerly

known as Adenoides eludens. *European Journal of Phycology* 50: 125–138.

GUILLARD R.R.L. & RYTHER J.H. 1962. Studies of marine planktonic diatoms. I. *Cyclotella nana* Hustedt and *Detonula confervacea* Cleve. *Canadian Journal of Microbiology* 8: 229–239.

HALL T.A. 1999. BioEdit: a user-friendly biological sequence alignment editor and analysis program for Windows 95/98/NT. pp. 95–98.

HARA Y. & HORIGUCHI T. 1982. A floristic study of the marine microalgae along the coast of the Izu Peninsula. *National Science Museum* 15: 99–108.

HERDMAN E.C. 1922. Notes on dinoflagellates and other organisms causing discolouration of the sand at Port Erin. II. *Proceedings and Transactions of the Liverpool Biological Society* 36: 15–30.

HOPPENRATH M. & ELBRÄCHTER M. 1998. *Roscoffia capitata* (Dinophyceae) refound: notes on morphology and biology. *Phycologia* 37: 450–457.

HOPPENRATH M. 2000a. Morphology and taxonomy of the marine sand-dwelling genus *Thecadinium* (Dinophyceae), with the description of two new species from the North German Wadden Sea. *Phycologia* 39: 96–108.

HOPPENRATH M. 2000b. An emended description of *Herdmania litoralis* Dodge (Dinophyceae) including the plate formula. *Nova Hedwigia* 3: 481–489.

HOPPENRATH M., SCHWEIKERT M. & ELBRACHTER M. 2003. Morphological reinvestigation and characterization of the marine, sand-dwelling dinoflagellate *Adenoides eludens* (Dinophyceae). *European Journal of Phycology* 38: 385–394.

HOPPENRATH M., HORIGUCHI T., MIYOSHI Y., SELINA M. & LEANDER B.S. 2007.

Taxonomy, phylogeny, biogeography, and ecology of *Sabulodinium undulatum* (Dinophyceae), including an emended description of the species. *Phycological Research* 55: 159–175.

HOPPENRATH M., YUBUKI N. , STERN R. & LEANDER B.S. 2017. Ultrastructure and molecular phylogenetic position of a new marine sand-dwelling dinoflagellate from British Columbia, Canada: *Pseudadenoides polypyrenoides* sp. nov. (Dinophyceae). *European Journal of Phycology* 52: 208–224.

KATOH K., KUMA K., TOH H. & MIYATA T. 2005. MAFFT version 5: improvement in accuracy of multiple sequence alignment. *Nucleic Acids Research* 33: 511–518.

LENAERS G., MAROTEAUX L., MICHOT B. & HERZOG M. 1989. Dinoflagellates in evolution. A molecular phylogenetic analysis of large subunit ribosomal RNA. *Journal of Molecular Evolution* 29**:** 40–51.

LEPERE C., DEMURA M., KAWACHI M., ROMAC S., PROBERT I. & VAULOT D. 2011. Whole-genome amplification (WGA) of marine photosynthetic eukaryote populations. *FEMS Microbiology Ecology* 76**:** 513–523.

LIU T., MERTENS K. & GU H. 2015a. Cyst–theca relationship and phylogenetic positions of the diplopsalioideans (Peridiniales, Dinophyceae),with description of *Niea* and *Qia* gen. nov. *Phycologia* 54: 210–232.

LIU T., MERTENS K.N., RIBEIRO S., ELLEGAARD M., MATSUOKA K. & GU H. 2015b. Cyst–theca relationships and phylogenetic positions of Peridiniales (Dinophyceae) with two anterior intercalary plates, with description of *Archaeperidinium bailongense* sp. nov. and *Protoperidinium fuzhouense* sp. nov. *Phycological*

*Research* 63: 134–151.

LUO Z., GU H., KROCK B. & TILLMANN U. 2013. *Azadinium dalianense*, a new dinoflagellate species from the Yellow Sea, China. *Phycologia* 52: 625–636.

MURRAY S. & PATTERSON D.J. 2002. *Amphidiniopsis korewalensis* sp. nov., a new heterotrophic benthic dinoflagellate. *Phycologia* 41: 382–388.

MURRAY S., HOPPENRATH M., PREISFELD A., LARSEN J., YOSHIMATSU S., TORIUMI S. & PATTERSON D.J. 2006. Phylogenetics of *Rhinodinium broomeense* gen. et. sp. nov., a peridinioid, sand-dwelling dinoflagellate (Dinophyceae). *Journal of Phycology* 42: 934–942.

ORR R.J.S., MURRAY S.A., STÜKEN A., RHODES L. & JAKOBSEN K.S. 2012. When naked became armored: An eight-gene phylogeny reveals monophyletic origin of theca in dinoflagellates. *PloS one* 7: e50004.

POSADA D. 2008. jModelTest: phylogenetic model averaging. *Molecular Biology and Evolution* 25: 1253–1256.

RONQUIST F. & HUELSENBECK J.P. 2003. MrBayes 3: Bayesian phylogenetic inference under mixed models. *Bioinformatics* 19: 1572–1574.

SABUROVA M., AL-YAMANI F. & POLIKARPOV I. 2009. Biodiversity of free-living flagellates in Kuwait's intertidal sediments. *BioRisk* 3: 97–110.

SABUROVA M. & CHOMÉRAT N. 2014. *Ailadinium reticulatum* gen. et sp. nov. (Dinophyceae), a new thecate, marine, sand-dwelling dinoflagellate from the northern Red Sea. *Journal of Phycology* 50: 1120–1136.

SALDARRIAGA J.F., TAYLOR F., KEELING P.J. & CAVALIER-SMITH T. 2001.

Dinoflagellate nuclear SSU rRNA phylogeny suggests multiple plastid losses and replacements. *Journal of Molecular Evolution* 53: 204–213.

SALDARRIAGA J.F., TAYLOR F.J.R.M., CAVALIER-SMITH T., MENDEN-DEUER S. & KEELING P.J. 2004. Molecular data and the evolutionary history of dinoflagellates. *European Journal of Protistology* 40: 85–111.

SCHOLIN C.A., HERZOG M., SOGIN M. & ANDERSON D.M. 1994. Identification of group-and strain-specific genetic markers for globally distributed *Alexandrium* (Dinophyceae). II. sequence analysis of a fragment of the LSU rRNA gene. *Journal of Phycology* 30**:** 999–1011.

SELINA M.S., CHOMÉRAT N. & HOPPENRATH M. 2015. Morphology and spatial distribution of *Cabra* species (Dinophyceae, Peridiniales) from Peter the Great Bay (northwestern Sea of Japan), including the description of *C. levis* sp. nov. *European Journal of Phycology* 50: 80–91.

SILVA, P. 1979. *Dinophyceae*. In Index Nominorum Genericorum (Plantarum) Vol. I. (Farr, E.R., Leussink, J.A. & Stafleu, F.A., eds.). Junk, Publishers, The Hague, The Netherlands.

STAMATAKIS A. 2006. RAxML-VI-HPC: maximum likelihood-based phylogenetic analyses with thousands of taxa and mixed models. *Bioinformatics* 22: 2688–2690.

TAKANO Y. & HORIGUCHI T. 2006. Acquiring scanning electron microscopical, light microscopical and multiple gene sequence data from a single dinoflagellate cell. *Journal of Phycology* 42: 251–256.

TAYLOR F.J.R. 1980. On dinoflagellate evolution. *Biosystems* 13**:** 65–108.

TILLMANN U., GOTTSCHLING M., NÉZAN E., KROCK B. & BILIEN G. 2014. Morphological and molecular characterization of three new *Azadinium* species (Amphidomataceae, Dinophyceae) from the Irminger Sea. *Protist* 165: 417–444.

TILLMANN U., BOREL C.M., BARRERA F., LARA R., KROCK B., ALMANDOZ G.O., WITT M. & TREFAULT N. 2016. *Azadinium poporum* from the Argentine Continental Shelf, Southwestern Atlantic, produces azaspiracid-2 and azaspiracid-2 phosphate. *Harmful Algae* 51: 40–55.

ZHANG H., BHATTACHARYA D. & LIN S. 2007. A three-gene dinoflagellate phylogeny suggests monophyly of Prorocentrales and a basal position for *Amphidinium* and *Heterocapsa*. *Journal of Molecular Evolution* 65: 463–474.

ZHU F., MASSANA R., NOT F., MARIE D. & VAULOT D. 2005. Mapping of picoeucaryotes in marine ecosystems with quantitative PCR of the 18S rRNA gene. *FEMS Microbiology Ecology* 52: 79–92.

## FIGURE CAPTIONS

Figs 1–6. LM of vegetative cells of *Adenoides sinensis* strain TIO303. Scale bars = 10 μm.

1. A living cell in ventral view showing the flattened body.

2. A living cell in right lateral view, showing the minute epitheca and the longitudinal flagellum (arrow).

3. A living cell in left lateral view, showing the minute epitheca and the transverse flagellum (arrows).

4. A living cell in lateral view, showing a small starch granule (arrow).

5. A living cell in right lateral view, showing a large starch granule (arrow).

6. A Sybr Green stained cell in lateral view showing a curved nucleus (N).

Figs 7–12. SEM of vegetative cells of *Adenoides sinensis* strain TIO303. Scale bars = 5 μm.

7. Apical view showing the pore plate (Po), apical plates (1′–5′), a ventral pore (arrow) and precingular plates (1″–6″).

8. Apical pore complex showing the pore plate (Po), a ventral pore (arrow), a cover plate (Cp) and a canal plate (X).

9. The same cell as in Fig. 8, showing the first apical plate (1′) and three precingular plates (4″–6″).

10. Apical view showing three precingular plates (1″–3″).

11. The same cell as in Fig. 8, showing an anterior sulcal plate (Sa), a left sulcal plate (Ss), a right sulcal plate (Sd) and a posterior sulcal plate (Sp).

12. Ventral view, showing an anterior sulcal plate (Sa), a left sulcal plate (Ss), a right sulcal plate (Sd) and a posterior sulcal plate (Sp).

Figs 13–21. SEM of vegetative cells of *Adenoides sinensis* strain TIO303. Scale bars = 5 μm.

13. Ventral view showing the two postcingular plates (1‴, 5‴) and two posterior intercalary plates (1p, 5p).

14. Ventral-lateral view, showing two posterior intercalary plates (1p, 2p).

15. Left-lateral view, showing two posterior intercalary plates (2p, 3p) and one postcingular plate (2‴).

16, 17. Dorsal view, showing two postcingular plates (2‴, 3‴) and two posterior intercalary plates (3p, 4p).

18. Right-lateral view, showing two posterior intercalary plates (4p, 5p) and one postcingular plate (4‴).

19. Dorsal-antapical view, showing two posterior intercalary plates (3p, 4p) and one antapical plate (1⁗).

20. Antapical view, showing one antapical plate (1⁗) and five posterior intercalary plates (1p–5p).

21. Detail of the dense pores in plates 3p, 4p and 1⁗.

Figs 22–30. SEM of vegetative cells of *Adenoides eludens* strain RCC1982. Scale bars = 5 μm.

22. Left-lateral view, showing two precingular plates (1″, 2″), three postcingular plates (1‴–3‴) and two posterior intercalary plates (1p, 2p).

23. Right-lateral view, showing two precingular plates (4″, 5″), three postcingular plates (3‴–5‴) and two posterior intercalary plates (2p, 3p).

24. Ventral view, showing two precingular plates (1″, 2″), three postcingular plates (1‴–3‴) and two posterior intercalary plates (1p, 3p).

25. Left-apical view, showing three precingular plates (1″–3″).

26. Right-apical view, showing three precingular plates (3″–5″).

27. Apical view, showing the pore plate (Po), five apical plates (1′–5′), and a ventral pore (arrow).

28. Apical view, showing the pore plate (Po), and a ventral pore (arrow).

29. Apical pore complex showing the pore plate (Po), a ventral pore (arrow), a cover plate (Cp) and a canal plate (X).

30. Ventral view showing an anterior sulcal plate (Sa), a left sulcal plate (Ss), a right sulcal plate (Sd) and a posterior sulcal plate (Sp).

Figs 31–40. Schematic interpretations of thecal plates of *Adenoides sinensis* and *A. eludens.*

31. Left-lateral view of *Adenoides sinensis*.

32. Dorsal view of *Adenoides sinensis*.

33. Right-lateral view of *Adenoides sinensis*.

34. Apical view of *Adenoides sinensis*.

35. Antapical view of *Adenoides sinensis*.

36. Left-lateral view of *Adenoides eludens*.

37. Dorsal view of *Adenoides eludens*.

38. Right-lateral view of *Adenoides eludens*.

39. Apical view of *Adenoides eludens*.

40. Antapical view of *Adenoides eludens*.

Fig. 41. A phylogenetic tree of *Adenoides sinensis* inferred from concatenated data of SSU and partial LSU rDNA sequences (2577 bases) using Bayesian inference. *Noctiluca scintillans* was selected as the outgroup. Branch lengths are drawn to scale, with the scale bar indicating the number of the substitutions per site. Numbers on branches are statistical support values to clusters on the right of them (Bayesian posterior probability / MLbootstrap support). Bootstrap values >50% and posterior probabilities above 0.8 are shown. * indicates maximal support (Bayesian posterior probability: 1.00/ ML bootstrap support: 100). Dashed lines indicate a half length. Clades are labeled and marked with vertical lines on the right. New sequences obtained in this study are indicated in bold font.

Figs S1–S6. SEM of vegetative cells of *Adenoides sinensis* strain TIO308. Scale bars = 5 μm.

1. Right-lateral view, showing the minute epitheca and large hypotheca.

2. Dorsal-apical view, showing the three apical plates (2′–4′), four precingular plates (2″–5″), the pore plate (Po) and cover plate (Cp).

3. Ventral view, showing the two apical plates (1′, 5′), the canal plate (X) and a pronounced ventral pore (arrow).

4. Ventral view showing the two postcingular plates (1‴, 5‴) and two posterior intercalary plates (1p, 5p).

5. Ventral view, showing an anterior sulcal plate (Sa), a left sulcal plate (Ss), a right sulcal plate (Sd) and a posterior sulcal plate (Sp).

6. Antapical view, showing one antapical plate (1⁗) and five posterior intercalary plates (1p–5p).

Figs S7–S10. LM of vegetative cells of *Adenoides eludens* strain RCC1982. Scale bars = 10 µm.

7. A living cell in lateral view, showing the transverse flagellum (arrows) and a nucleus (N).

8. A living cell in lateral view, showing the transverse flagellum (arrowhead), the longitudinal flagellum (arrow) and a large food vacule (F).

9. A living cell in lateral view, showing a presumably pyrenoid (P) surrounded by a starch ring.

10. A living cell in lateral view, showing a presumably single chloroplast connecting to form a network.

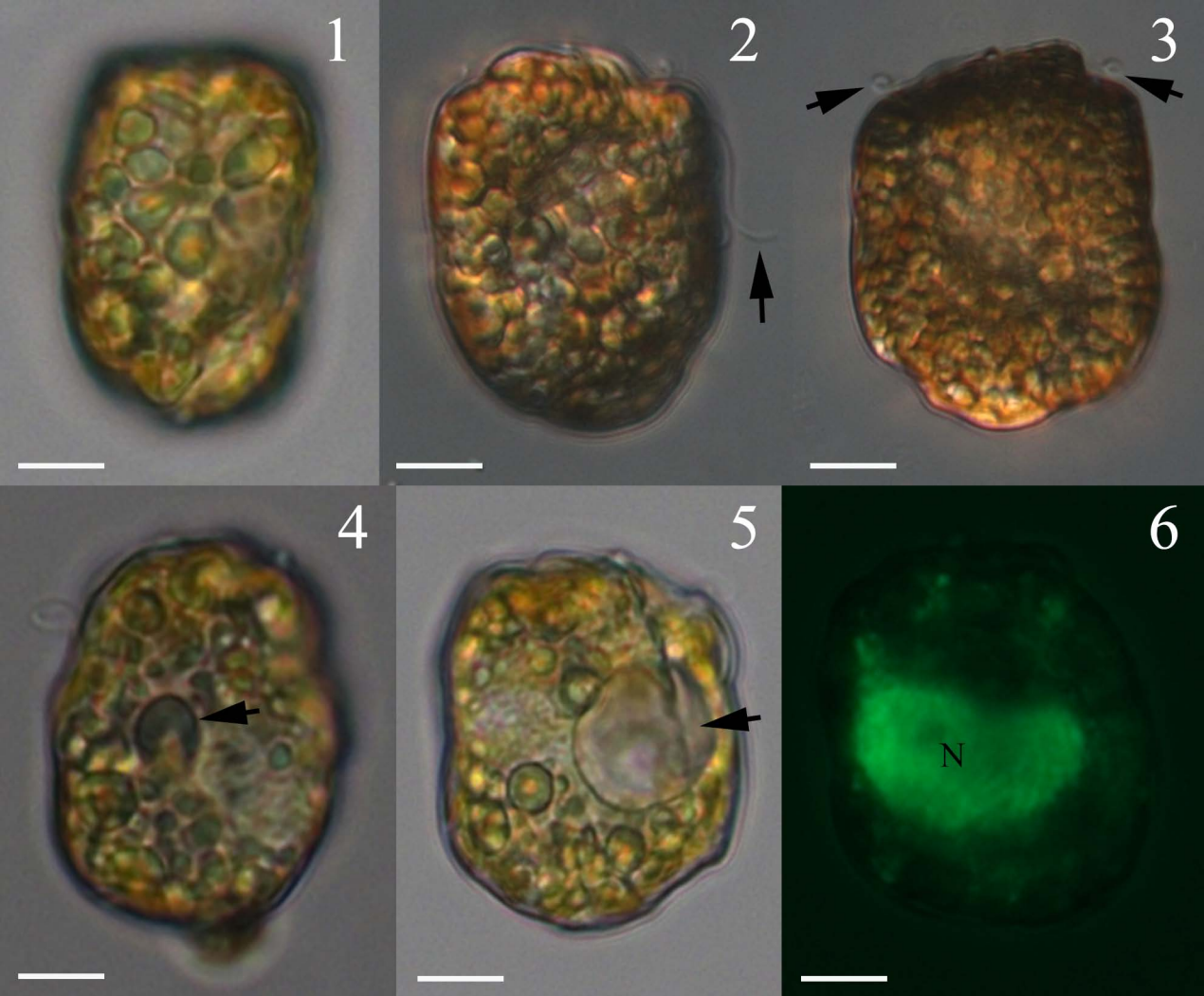
1
2
3
4
5
6
N

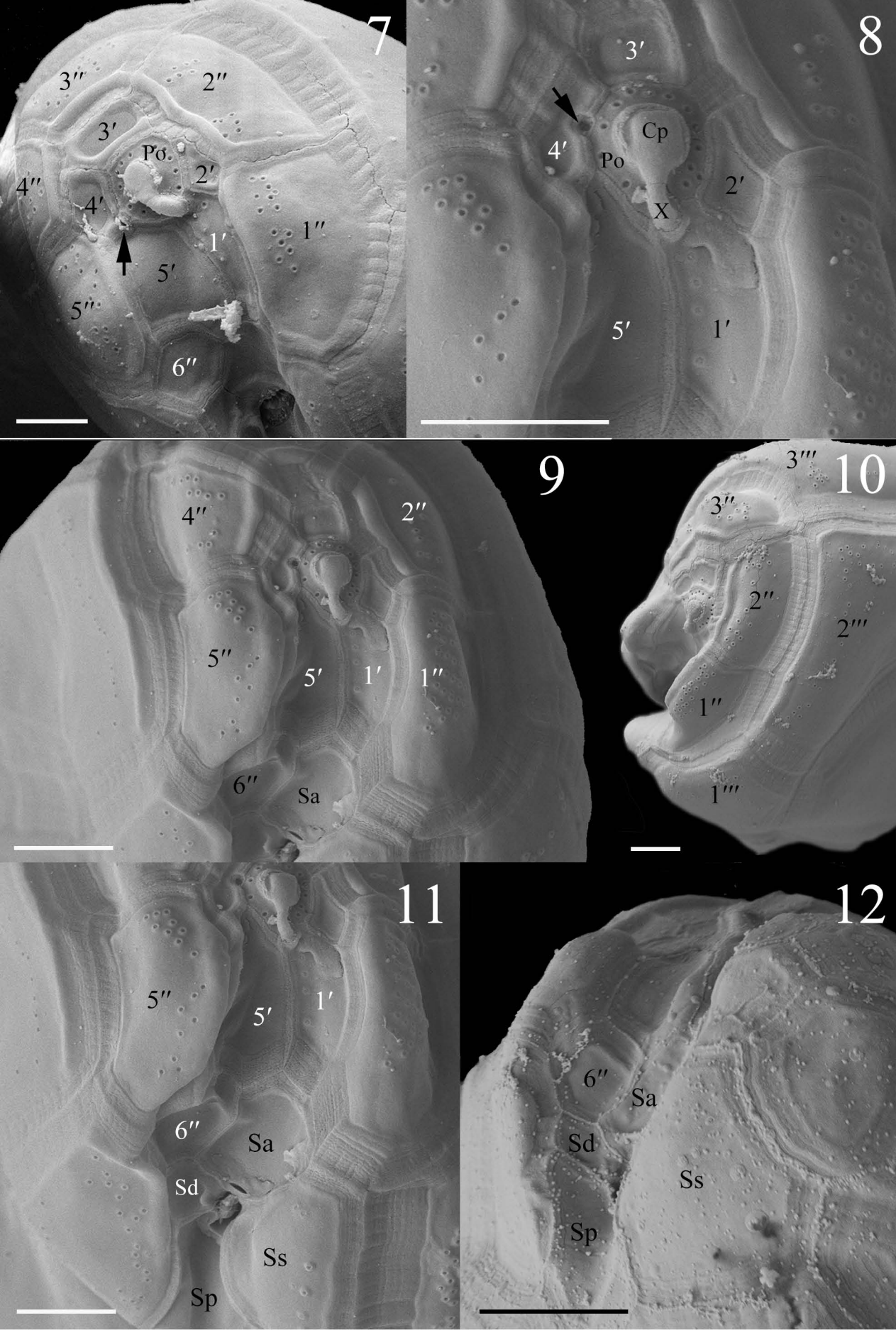
7
3″
2″
3′
Po
2′
4″
4′
1′
1″
5′
5″
6″
8
3′
Cp
4′
Po
2′
X
5′
1′
9
4″
2″
5″
5′
1′
1″
6″
Sa
10
3‴
3″
2″
2‴
1″
1‴
11
5″
5′
1′
6″
Sa
Sd
Ss
Sp
12
6″
Sa
Sd
Ss
Sp

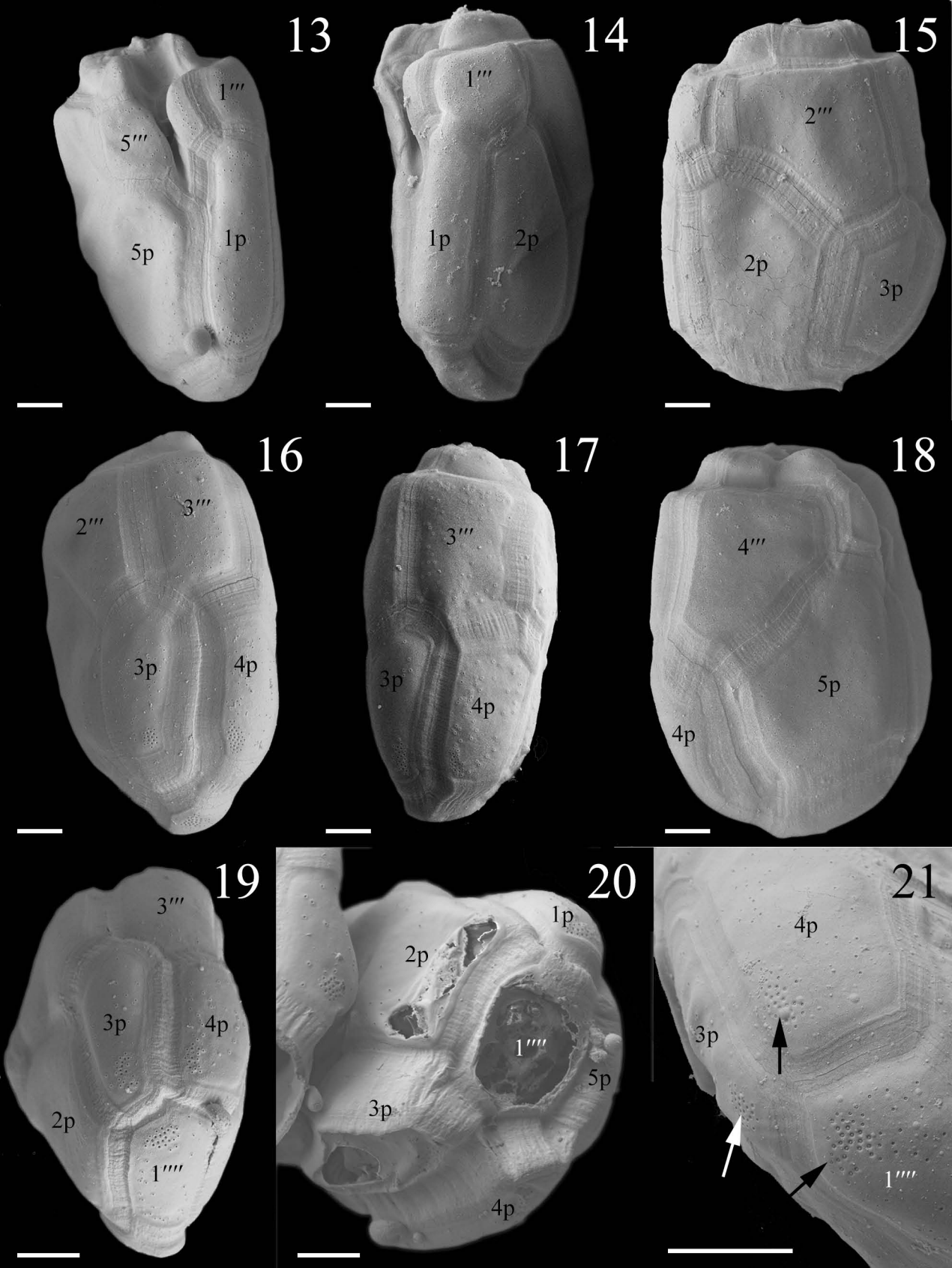
13
1‴
5‴
5p
1p
14
1‴
1p
2p
15
2‴
2p
3p
16
2‴
3‴
3p
4p
17
3‴
3p
4p
18
4‴
5p
4p
19
3‴
3p
4p
2p
1⁗
20
1p
2p
1⁗
5p
3p
4p
21
4p
3p
1⁗

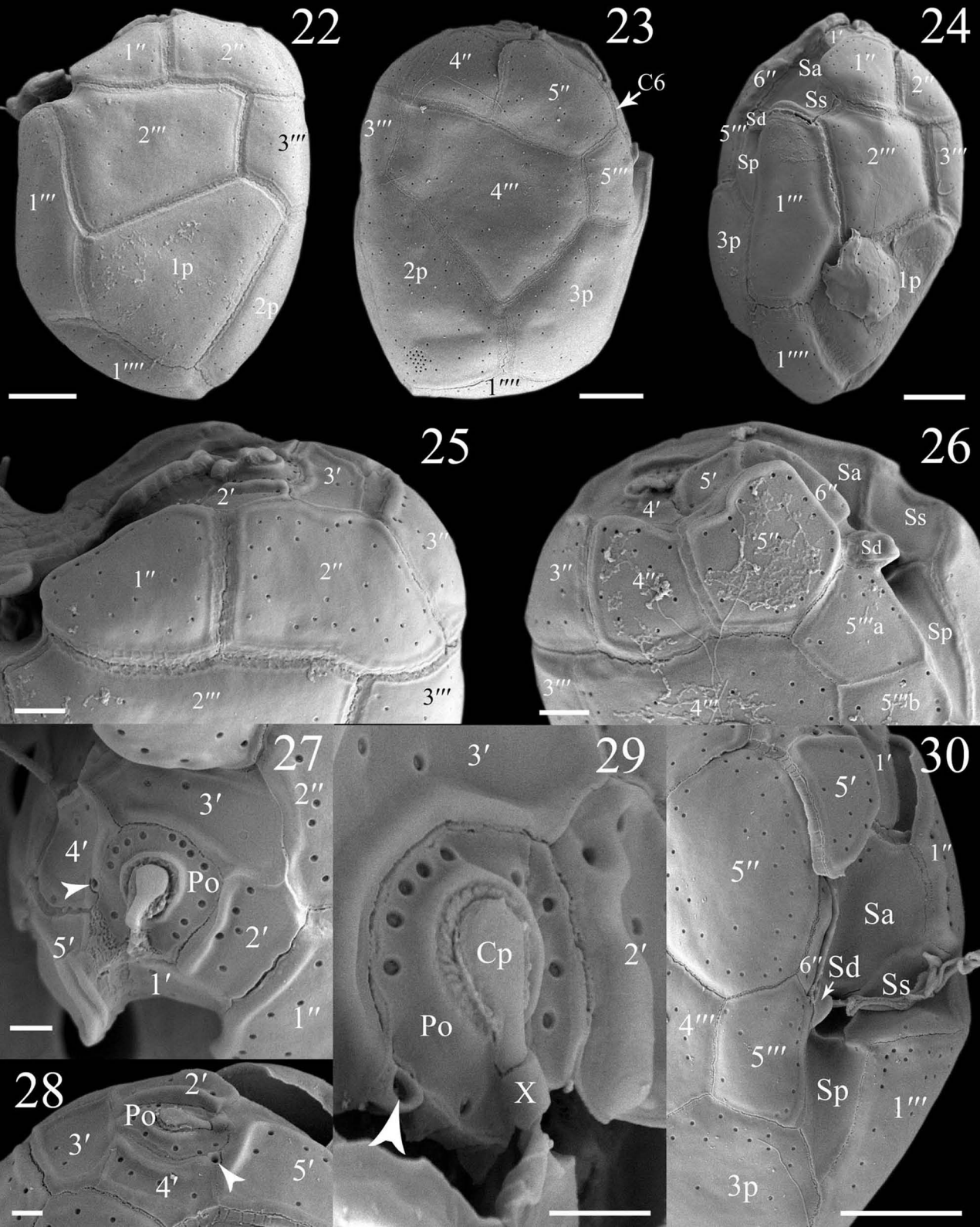
22
1″
2″
2‴
3‴
1‴
1p
2p
1⁗
23
4″
5″
C6
3‴
4‴
5⁗
2p
3p
1⁗
24
1′
6″
Sa
1″
2″
Ss
Sd
5⁗
Sp
2‴
3‴
1‴
3p
1p
1⁗
25
2′
3′
3″
1″
2″
2‴
3‴
26
5′
Sa
6″
4′
Ss
5″
Sd
3″
4‴
5‴a
Sp
3‴
4⁗
5⁗b
27
3′
2″
4′
Po
5′
2′
1′
1″
28
2′
Po
3′
4′
5′
29
3′
Cp
2′
Po
X
30
1′
5′
1″
5″
Sa
6″
Sd
Ss
4⁗
5‴
Sp
1‴
3p

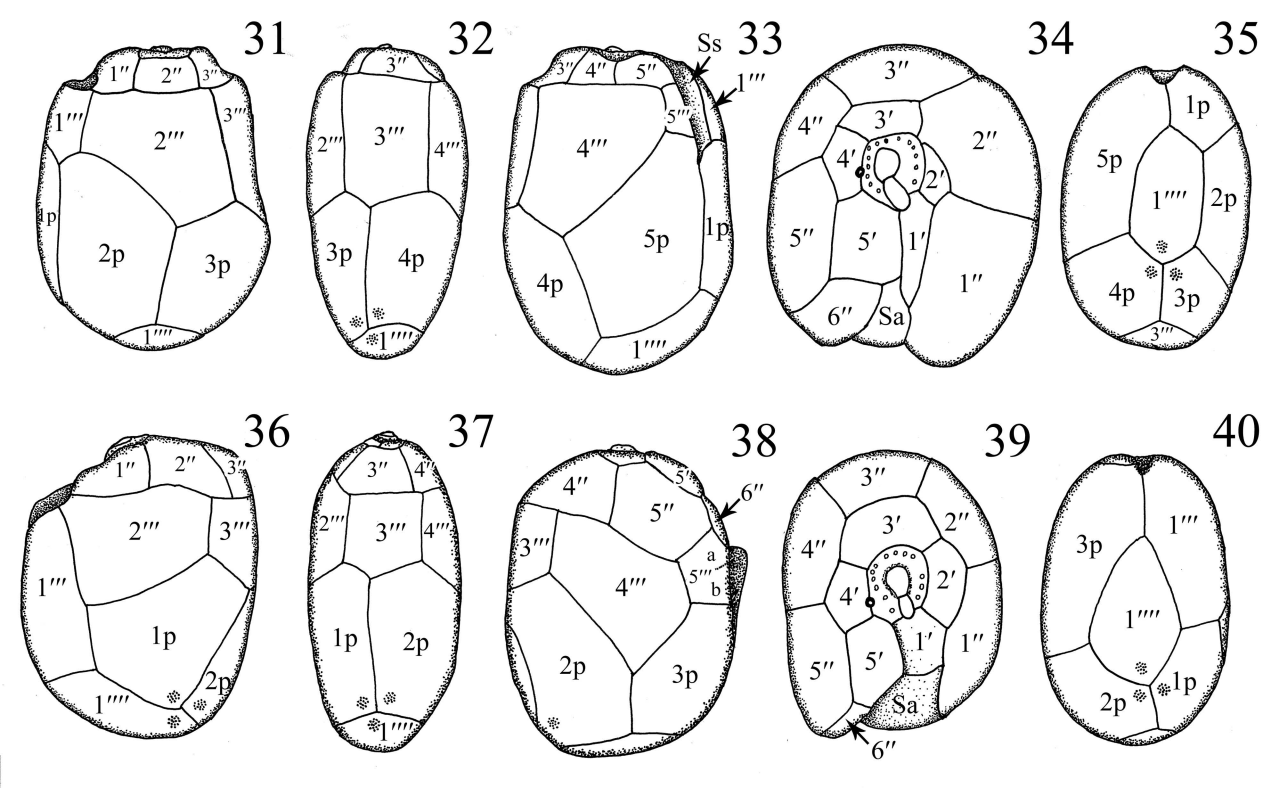
31
1″
2″
3″
1‴
2‴
3‴
1p
2p
3p
1⁗
32
3″
2‴
3‴
4‴
3p
4p
1⁗
33
Ss
3″
4″
5″
1‴
5‴
4‴
5p
1p
4p
1⁗
34
3″
4″
3′
4′
2′
2″
5″
5′
1′
1″
6″
Sa
35
1p
5p
1⁗
2p
4p
3p
3‴
36
1″
2″
3″
2‴
3‴
1‴
1p
2p
1⁗
37
3″
4″
2‴
3‴
4‴
1p
2p
1⁗
38
4″
5′
5″
6″
3‴
a
5‴
b
4‴
2p
3p
39
3″
3′
2″
4″
4′
2′
1′
1″
5″
5′
Sa
6″
40
3p
1‴
1⁗
2p
1p

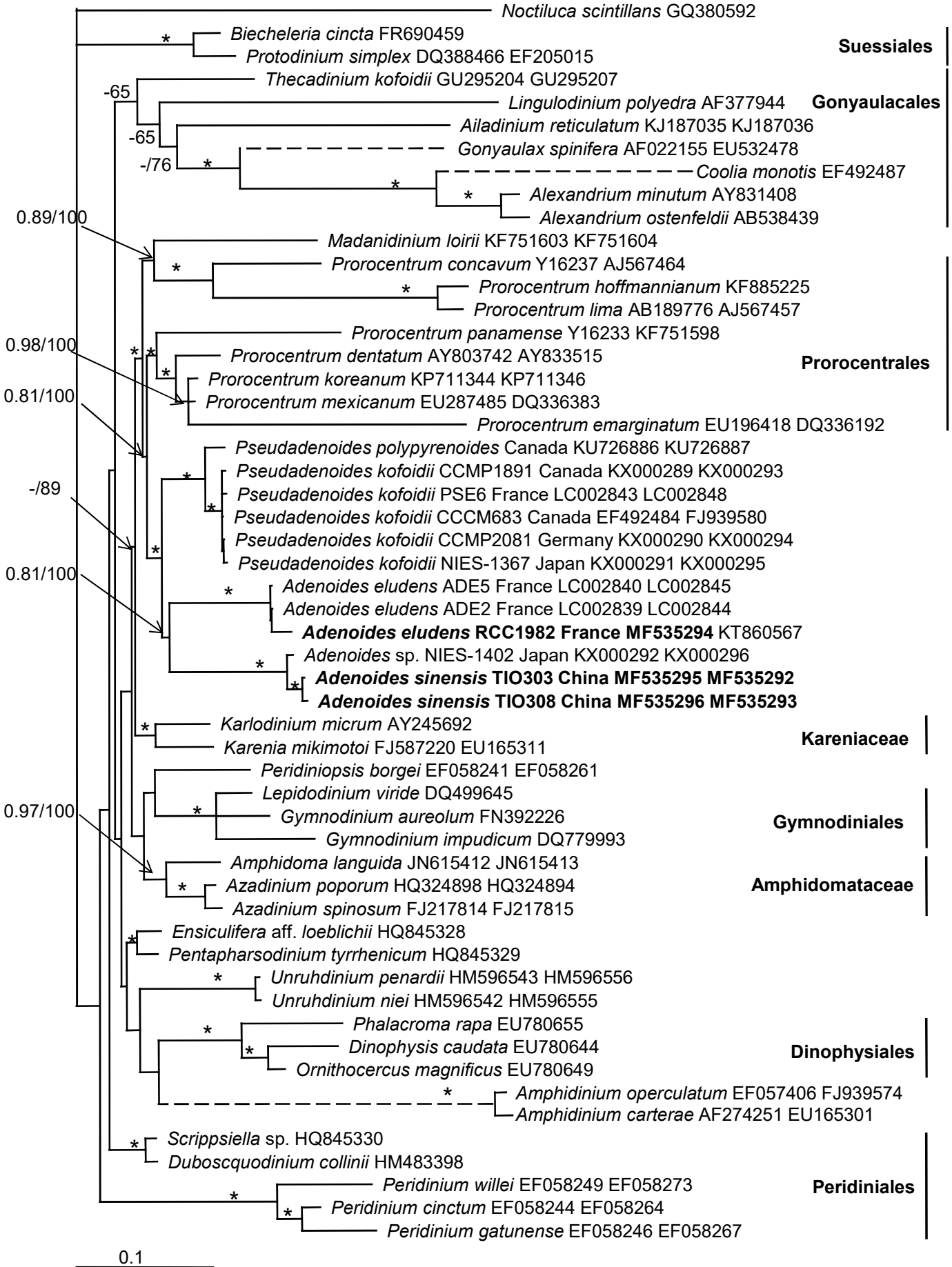
Noctiluca scintillans GQ380592
Biecheleria cincta FR690459
Protodinium simplex DQ388466 EF205015
Suessiales
Thecadinium kofoidii GU295204 GU295207
Lingulodinium polyedra AF377944
Gonyaulacales
Ailadinium reticulatum KJ187035 KJ187036
Gonyaulax spinifera AF022155 EU532478
Coolia monotis EF492487
Alexandrium minutum AY831408
Alexandrium ostenfeldii AB538439
Madanidinium loirii KF751603 KF751604
Prorocentrum concavum Y16237 AJ567464
Prorocentrum hoffmannianum KF885225
Prorocentrum lima AB189776 AJ567457
Prorocentrum panamense Y16233 KF751598
Prorocentrum dentatum AY803742 AY833515
Prorocentrum koreanum KP711344 KP711346
Prorocentrum mexicanum EU287485 DQ336383
Prorocentrum emarginatum EU196418 DQ336192
Prorocentrales
Pseudadenoides polypyrenoides Canada KU726886 KU726887
Pseudadenoides kofoidii CCMP1891 Canada KX000289 KX000293
Pseudadenoides kofoidii PSE6 France LC002843 LC002848
Pseudadenoides kofoidii CCCM683 Canada EF492484 FJ939580
Pseudadenoides kofoidii CCMP2081 Germany KX000290 KX000294
Pseudadenoides kofoidii NIES-1367 Japan KX000291 KX000295
Adenoides eludens ADE5 France LC002840 LC002845
Adenoides eludens ADE2 France LC002839 LC002844
Adenoides eludens RCC1982 France MF535294 KT860567
Adenoides sp. NIES-1402 Japan KX000292 KX000296
Adenoides sinensis TIO303 China MF535295 MF535292
Adenoides sinensis TIO308 China MF535296 MF535293
Karlodinium micrum AY245692
Karenia mikimotoi FJ587220 EU165311
Kareniaceae
Peridiniopsis borgei EF058241 EF058261
Lepidodinium viride DQ499645
Gymnodinium aureolum FN392226
Gymnodinium impudicum DQ779993
Gymnodiniales
Amphidoma languida JN615412 JN615413
Azadinium poporum HQ324898 HQ324894
Azadinium spinosum FJ217814 FJ217815
Amphidomataceae
Ensiculifera aff. loeblichii HQ845328
Pentapharsodinium tyrrhenicum HQ845329
Unruhdinium penardii HM596543 HM596556
Unruhdinium niei HM596542 HM596555
Phalacroma rapa EU780655
Dinophysis caudata EU780644
Ornithocercus magnificus EU780649
Dinophysiales
Amphidinium operculatum EF057406 FJ939574
Amphidinium carterae AF274251 EU165301
Scrippsiella sp. HQ845330
Duboscquodinium collinii HM483398
Peridinium willei EF058249 EF058273
Peridinium cinctum EF058244 EF058264
Peridinium gatunense EF058246 EF058267
Peridiniales
-65
-65
-/76
0.89/100
0.98/100
0.81/100
-/89
0.81/100
0.97/100
0.1

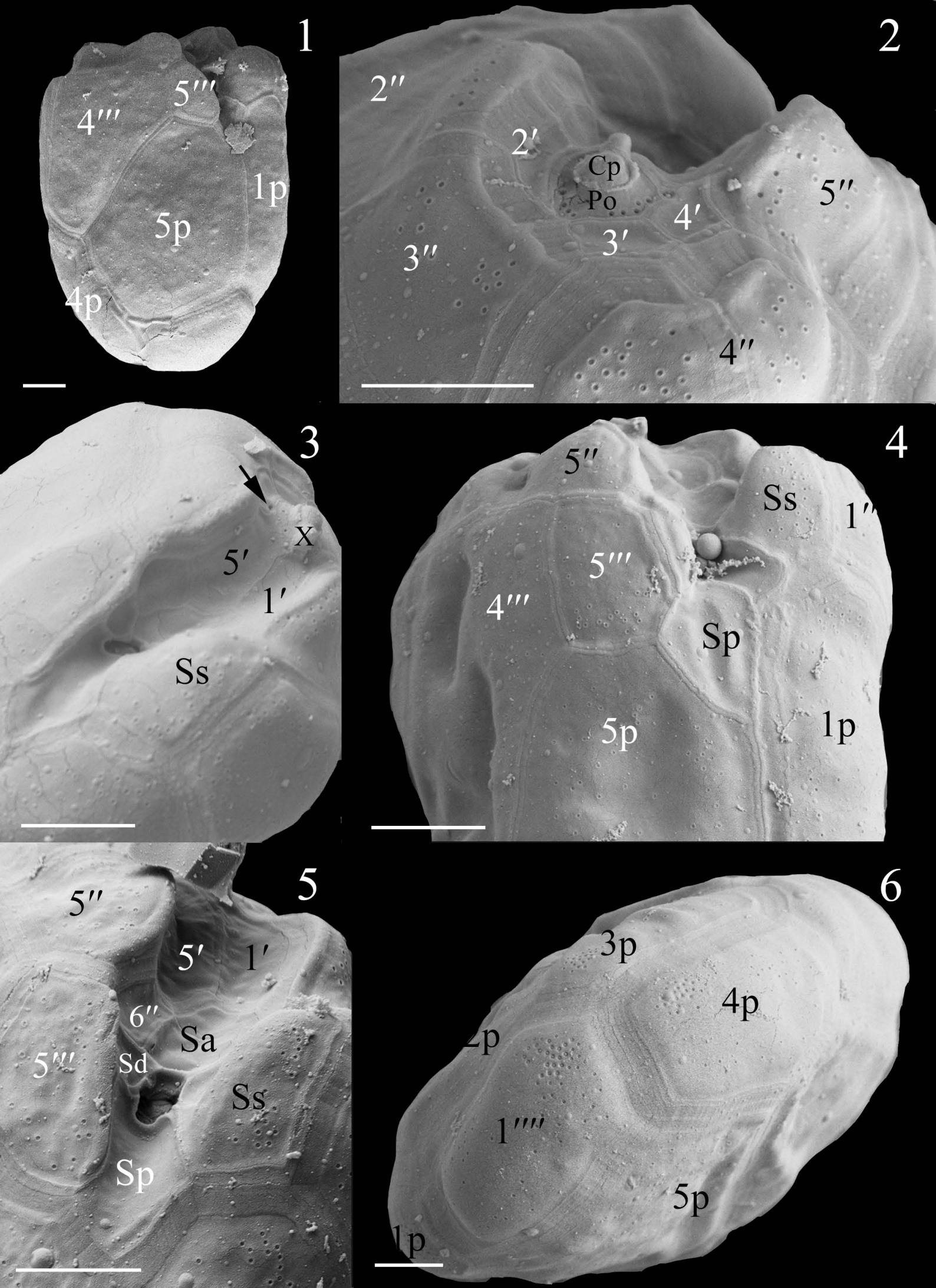
1
5‴
4‴
1p
5p
4p
2
2″
2′
Cp
Po
5″
4′
3′
3″
4″
3
X
5′
1′
Ss
4
5″
Ss
1″
5‴
4‴
Sp
5p
1p
5
5″
5′
1′
6″
Sa
5‴
Sd
Ss
Sp
6
3p
4p
2p
1‴‴
5p
1p

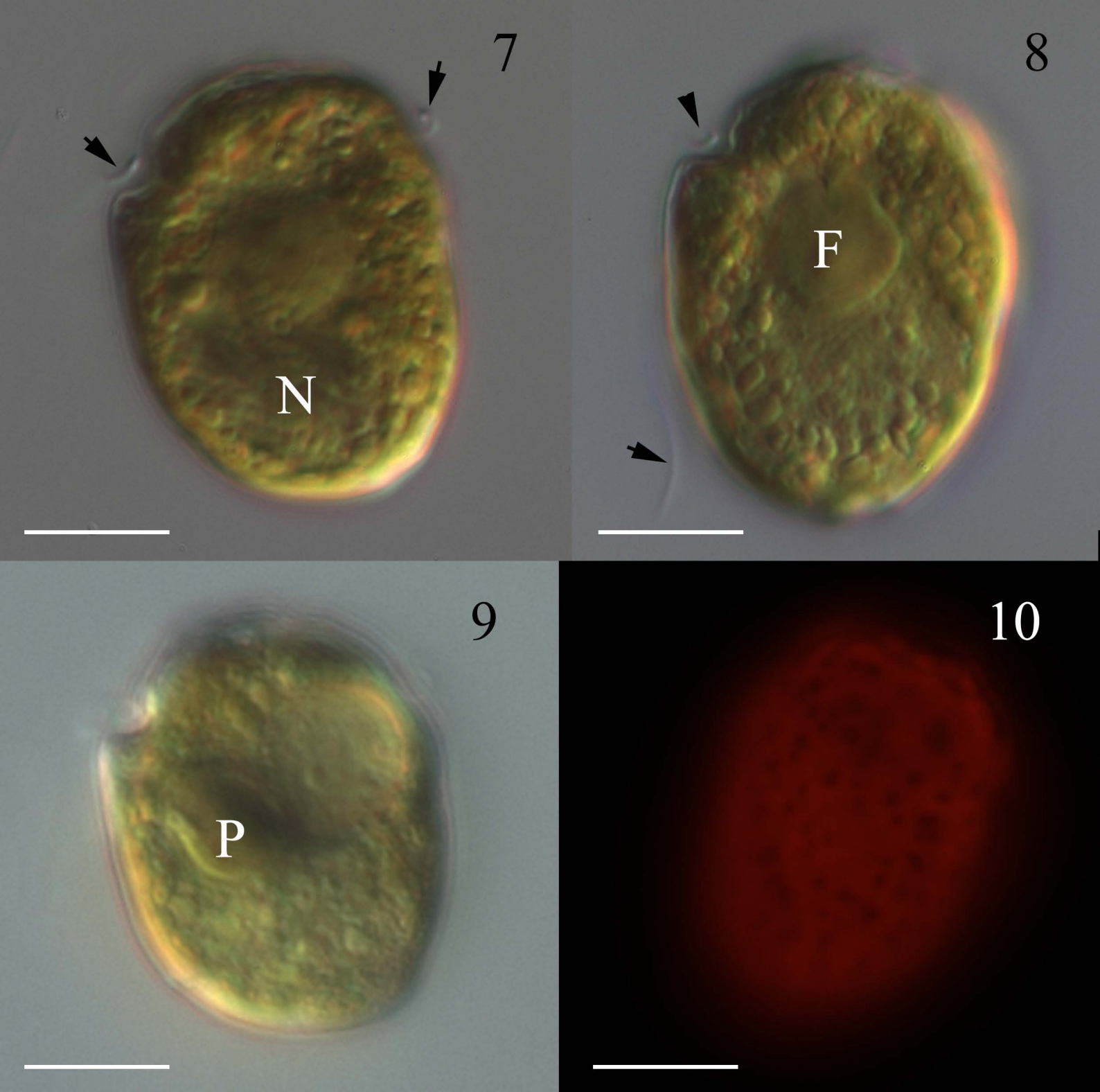
7
N
8
F
9
P
10